Collisionless Laser Beam Absorption: Models, present understanding, fast electron spectra, regimes and scaling laws

P. Mulser[1], S.M. Weng[2], K. Murakami[2]

[1] *TQE: Theoretical Quantum Electronics, Technical University, Darmstadt, Germany*

[2] *ILE: Institute of Laser Engineering, Osaka University, Osaka, Japan*

Present understanding

During the last three decades collisionless absorption of intense fs laser pulses in solid targets has been intensively studied by experiments, numerical simulations and analytic theory. Though electron ion collisions are almost absent, degrees of absorption have been found as high as 95% (see e.g. [1]). The author presents a rather complete collection of values from numerous labs obtained until recently. Not only vary the data considerably from intensity to intensity, but also at fixed laser intensity the results scatter strongly, e. g., from 35 to 80% at $I = 6 \times 10^{18}$ W cm^{-2} and angle of incidence $\alpha = 45^{\circ}$. It indicates that collisionless absorption is a very complex phenomenon, accessible to a quantitative analysis perhaps only via numerical simulations. Such approach, like experiments, needs interpretation. It is therefore essential to gain a qualitative picture of the leading physical processes by which collisionless absorption is accomplished. To this aim numerous models of different type have been proposed , discussed e.g. in [1-3] , nevertheless physical understanding has not yet reached a satisfactory level. Among this variety the models by F. Brunel [4], non-relativistic, and P. Gibbon [6], fully relativistic energy-momentum tensor based, deserve particular attention for their conceptual simplicity and logical coherence. A detailed analysis of Brunel's model [4] is given in [5]. Our investigations presented in the following will show that essential building blocks are still missing. To make further progress in conceptual understanding, one-dimensional (1D) numerical simulations, in the sub-relativistic domain even with the ions held fixed, and restricted to short times (no appreciable rarefaction of the ion fluid) are justified at present. In particular, we shall show that resonant laser-particle interaction and mutual influence of the fast electron jets and return currents will have a strong impact on the electron energy spectra and their "temperature"-intensity scaling. In what follows the shortcomings of Brunel's model are listed, then the question of the electron spectra *in statu nascendi* and their temporal evolution and mixing with the cold electron fluid are investigated and the present understanding of scaling relations is discussed. The findings may have an impact on how to improve further Gibbon's fully relativistic absorption model.

Brunel's absorption model and anharmonic resonance

A plane wave impinges under angle α from the vacuum onto a flat overdense target, with component normal to to its surface (x direction) $E(\tau) = E_o \sin\tau, \tau = \omega t$, pulls the electrons from the surface layer into the vacuum and pushes them back to the field-free target interior. The dynamics of an electron layer at position x_l is governed by the the dimensionless velocity $w_l(\tau) = v_l/v_{os}$ and the space coordinate $s_l(\tau) = x_l(\tau)\omega/v_{os}$, v_{os} quiver velocity amplitude [5],

$$w_l(\tau) = (\cos\tau - \cos\tau_l) + (\tau - \tau_l)\sin\tau_l; \quad \tau \geq \tau_l,$$

$$s_l(\tau) = (\sin\tau - \sin\tau_l) - (\tau - \tau_l)\cos\tau_l + \frac{1}{2}(\tau - \tau_l)^2 \sin\tau_l + \frac{x_{0l}\omega}{v_{os}}; \quad \tau \geq \tau_l.$$

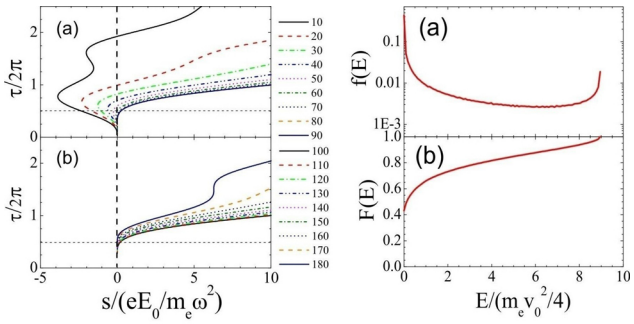

Figure 1: Brunel model. LHS: Electron orbits, RHS: Energy spectrum

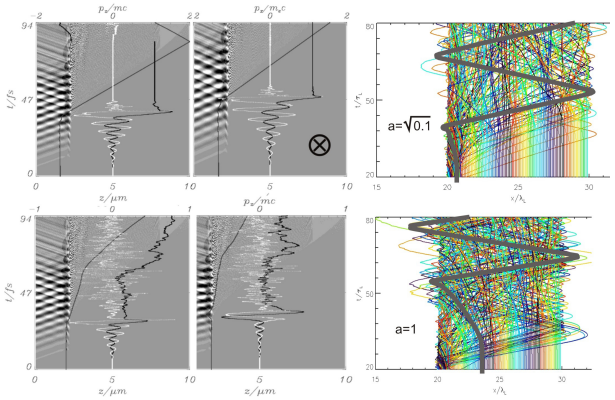

Figure 2: Energy gain by anharmonic resonance, $I = 10^{17}$ W/cm^2, mobile ions. LHS: 4 orbits undergoing resonance in the laser field (regular shadow strucure) and subsequent modifications by plasmons. $p_x(t)/m_e c$ normalized electron momentum, white line: total electric field at electron position. x electron gains $23.5 \times E_{os}$. RHS: Selection of 10^3 orbits at $a = 0.1$ and $a = 1.0$. Bold orbits: resonance is strongest.

The orbits $s_l(\tau)$ are shown in Fig. 1(a), left. Note that only during $\tau \leq \pi/2 + 2n\pi$ layers are pulled into the vacuum, at all later instants of a laser cycle layers would move into the target interior (see Fig. 1(b), left, which is not possible owing to complete screening of the laser field. The motion of all relevant layers shows periodicity 2π, and no crossing of layers takes place. The energy spectrum $f(E)$ and its integral $F(E) = \int f(E)dE$ of the electrons is depicted on the RHS (a), (b). f, F are universal, i.e., they are independent of the laser intensity. The energy spectrum shows a pronounced cut off at $E_{max} = 9.07 \times E_{os}$, E_{os} mean oscillation energy in vacuum. Contrary to a general belief, electrons pulled into the vacuum at $\tau > \pi/4$ and $\tau = \pi/2$ are not pushed back by the laser field, they *fall* back attracted by their space charge against

the laser field. This leads to a separation of the electron spectrum $f(E)$ into high and low energies. Shortcomings of Brunel's model are no return current dynamics, no crossing of electron orbits, excluding in this way resonant interaction with the laser driver and breaking of electron fluid flow ("wave breaking"), too high number of fast electrons, i.e., above E_{os} ($\gtrsim 40\%$) [5].

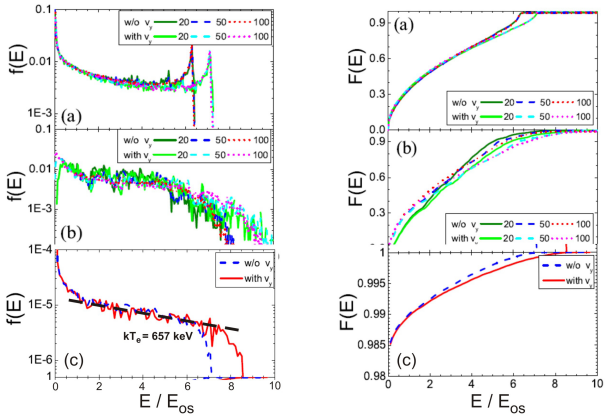

Figure 3: Evolution of electron spectrum $f(E)$, $F(E)$ from *statu nascendi*, (a), (b) after 20, 50 and 100 fs; (c) after 100 fs. Hydrogen target, 100 times overdense, 50 ţm thick, constant $a = 1.0$ pulse, 45° incidence, fixed ions.

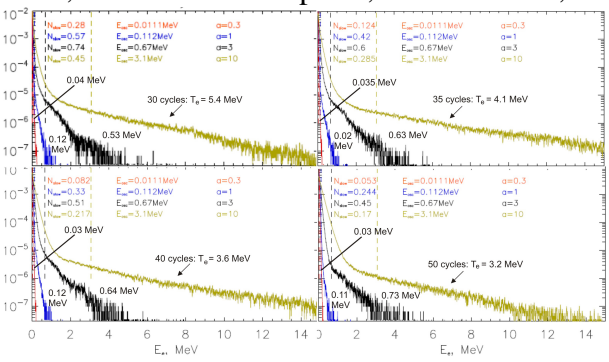

Figure 4: Gaussian laser pulse of $FHW = 50$ cycles Nd, $a = 0.31, 1.0, 3.16, 10$, 45° incidence. Evolution of Maxwellian tail in time and concomitant electron "temperatures" T_e.

In Fig. 2 electron orbits $x(t)$ from 1D particle-in-cell(PIC) simulations are shown. Anharmonic resonance is recognized from the abrupt change of the slope and from the change of momentum p [7]. In contrast to [4] the electrons undergo several oscillations before going through resonance statistically. The pictures on the RHS of 2 for $a = eA/m_e c = 0.1$ and 1.0 show that the phase shift in the resonance leads to orbit crossing, intense electron fluid mixing and breaking of regular flow ("wave breaking"). The jets of fast electrons generate plasmons which in turn act back on the jets and lead to particle trapping, strong fast electron-return current coupling and collective heating of the bulk plasma.

Electron spectrum *in statu nascendi***?**

The fast electron spectra from experiments, and also from simulations, are modified by numerous collisions. It would be of principal interest to know $f(E)$ of the electrons just after having interacted for the first time with the laser field, t.e., *in statu nascendi*. In simulations this is possible. In Fig. 3(a) energy spectrum of electrons re-entering the target up to time 20, 50, 100 fs with energy from v_x only (lower cut off) and from v_x and v_y; (b) the same electrons when crossing the target interior at $x = 2$ wavelengths.

Beginning of Maxwellization is noticeable. (c) shows the spectrum of all electrons at $t = 100$ fs. It shows the building up of a Maxwellian tail of electron "temperature" $T_e = 657$ keV and the reduction of the fraction of fast electrons to the order of 1%. The partial evolution of of the hot electrons into a Maxwellian distribution is studied further in PIC with a Gaussian laser pulse of 4 different intensities, see Fig. 4. Again, the fraction of hot electrons is as low as in Fig. 3(c). The evolution of T_e in time depends on the intensity.

Statistics and Conclusions

From the PIC simulations with the target of Fig. 3 and laser pulse constant in time the fraction of the number and the mean energy as well as the electron density n_{eff} at which the interaction with the laser occurs most effectively and the true mean kinetic electron temperature are given at $t = 100$ fs. Contrary to the general assumption n_{eff} is much lower than the critical density n_c. So far we have shown

- Fast electrons are generated first: anharmonic resonance $\Rightarrow$ breaking of regular flow
- Strong interaction of fast electron jets with return current: collective heating of bulk plasma
- Non-Maxwellian electron distribution, partially evolving into Maxwellian tail
- Effective mean interaction density $n_{eff} << n_c$ is a strongly decreasing function of intensity $\Rightarrow$ impact on energy scaling
- No universal scaling relations: different quantities scale differently with laser intensity.

a= eA / m_ec	I [Wcm^{-2}]	N_{ehot}	E_{ehot}	n_{eff} /n_c	kT_e /E_{tot}
1.0	1.4 x 10^{18}	12.2 %	62 %	0.18	0.69
$\sqrt{10}$	1.4 x 10^{19}	4.1 %	21.5 %	0.19	0.24
$10\sqrt{10}$	1.4 x 10^{21}	0.76 %	2.6 %	4.2x10^{-3}	0.16

Figure 5: Fraction of number of hot electrons N_{ehot}, energy fraction E_{ehot}, effective absorption density n_{eff} and relativistic kinetic temperature after 100fs.

Acknowledgement First author likes to acknowledge generous support by the European Science Foundation ESF.

[1] J.R. Davies, Plasma Phys. Contr. Fusion **51**, 014006 (2009)

[2] P. Mulser, D. Bauer, *High-Power Laser-Matter Interaction*, Springer, Heidelberg (2010)

[3] D. Bauer, P. Mulser, Phys. Plasmas **14**, 023301 (2007)

[4] F. Brunel, Phys. Rev. Lett. **59**, 52 (1987)

[5] P. Mulser, S.M. Weng and Tatyana Liseykina, Phys. Plasmas **19**, 043301 (2012)

[6] P. Gibbon, A. Andreev, K. Platonov, Plasma Phys. Contr. Fusion **54**, 045001 (2012)

[7] P. Mulser, D. Bauer, and H. Ruhl, Phys. Rev. Lett **101**, 225002 (2008)